Cerebral Cortex October 2015;25:3682–3689
doi:10.1093/cercor/bhu220
Advance Access publication September 26, 2014

Thalamic Involvement in Fluctuating Cognition in Dementia with Lewy Bodies: Magnetic Resonance Evidences

Stefano Delli Pizzi[1,2,3], Raffaella Franciotti[1,2,3], John-Paul Taylor[4], Astrid Thomas[1,2], Armando Tartaro[1,3], Marco Onofrj[1,2] and Laura Bonanni[1,2]

[1]Department of Neuroscience, Imaging and Clinical Sciences, [2]Aging Research Centre, Ce.S.I. and [3]Institute for Advanced Biomedical Technologies (ITAB), "G. d'Annunzio" University, Chieti, Italy and [4]Institute for Ageing and Health, Newcastle University, Campus for Ageing and Vitality, Newcastle upon Tyne NE4 5PL, UK

Address correspondence to Laura Bonanni, Department of Neuroscience, Imaging and Clinical Sciences, G. d'Annunzio University of Chieti-Pescara, Via dei Vestini, 66100 Chieti, Italy. Email: l.bonanni@unich.it

Dementia with Lewy bodies (DLB) is characterized by fluctuation in cognition and attention. Thalamocortical connectivity and integrity of thalami are central to attentional function. We hypothesize that DLB patients with marked and frequent fluctuating cognition (flCog) have a loss of thalamocortical connectivity, an intrinsic disruption to thalamic structure and imbalances in thalamic neurotransmitter levels. To test this, magnetic resonance imaging (MRI), diffusion tensor imaging (DTI) and proton MR spectroscopy on thalami were performed on 16 DLB, 16 Alzheimer's disease (AD) and 13 healthy subjects. MRI and DTI were combined to subdivide thalami according to their cortical connectivity and to investigate microstructural changes in connectivity-defined thalamic regions. Compared with controls, lower *N*-acetyl-aspartate/total creatine (NAA/tCr) and higher total choline/total creatine (tCho/tCr) values were observed within thalami of DLB patients. tCho/tCr increase was found within right thalamus of DLB patients as compared with AD. This increase correlated with severity and frequency of flCog. As compared with controls, DLB patients showed bilateral damage within thalamic regions projecting to prefrontal and parieto-occipital cortices, whereas AD patients showed bilateral alteration within thalamic region projecting to temporal cortex. We posit that microstructural thalamic damage and cholinergic imbalance may be central to the etiology of flCog in DLB.

Keywords: attention, choline, dementia with Lewy bodies, fluctuating cognition, thalamus

Introduction

The thalamus plays a central role in altering and maintaining arousal (Steriade 2006; Ward 2011). Anatomically, its nuclei are topographically organized to modulate and synchronize distributed cortical networks supporting large-scale cerebral dynamics related to goal-directed behaviors and awareness (Schiff 2008). On this basis, it was suggested that phenomenal consciousness is generated by synchronized neural activity in thalamic neurons and that thalamic activity is driven by information arising from the cortical computation (Ward 2011).

Abnormal functional connectivity and microstructural damage within thalami have been previously reported in dementia with Lewy bodies (DLB) (Watson et al. 2012; Kenny et al. 2013). DLB patients were clinically characterized by spontaneous alteration in cognition, attention, and arousal (Lee et al. 2012). These symptoms were reported as fluctuating cognition (flCog), which represents, together with visual hallucinations and extrapyramidal signs, the core clinical features of DLB (McKeith et al. 2005).

Several neuroimaging studies have focused on the neural bases of flCog in DLB patients, suggesting a relation between the severity of flCog and covariant perfusional network changes (Taylor et al. 2013) or functional magnetic resonance imaging (fMRI) blood oxygen-dependent level (BOLD) (Franciotti et al. 2013; Peraza et al. 2014) alterations. In addition, increased thalamic perfusion on single photon emission computed tomography (SPECT) (O'Brien et al. 2005) and changes in dopaminergic and cholinergic systems within thalami have been linked to flCog in DLB (Pimlott et al. 2006; Piggott et al. 2007). Of note, the cholinergic system is widely distributed in the brain and it is more affected in DLB than in Alzheimer's disease (AD) patients (Kotagal et al. 2012). This concept is amply supported by pharmacological evidences which suggest that (1) anticholinergic drugs can induce a symptom profile of altered arousal comparable to flCog in DLB (Perry et al. 1999) and (2) cholinesterase inhibitors can significantly improve flCog and attentional function in DLB (McKeith et al. 2000; Onofrj et al. 2003; Wesnes et al. 2005).

Based on these considerations and on the central role of thalamic neurons in regulating arousal and attention, we hypothesized that cholinergic imbalance within thalami and damage of the structural connectivity between thalami and cortical regions modulating alertness and attention are associated with flCog in DLB.

To test this, we carried out a study using multimodal techniques including structural magnetic resonance imaging (MRI), diffusion tensor imaging (DTI) and proton MR Spectroscopy (^{1}H-MRS) in a cohort of DLB and AD patients as well as healthy controls. ^{1}H-MRS technique assesses, in vivo, different metabolites such as *N*-acetyl-aspartate (NAA) and total choline (tCho) which are specifically related to decrease of neuronal integrity and to cholinergic deficits respectively. The combination of structural MRI and DTI allows parcellation of the thalami according to their cortical structural connectivity and to investigate microstructural integrity in each connectivity-defined region. The comparison between DLB and AD was performed to assess whether any possible structural and metabolic changes in the thalami were specific of a dementia characterized by the presence of flCog (DLB) or more as a result of a process of dementia per se. Furthermore, the variation of severity and frequency of flCog among DLB patients provides a means by which to assess whether the MR thalamic changes are associated with more overt flCog.

Material and Methods

Study Sample

This study was approved by Local Institutional Ethics Committee. All participants (or their caregivers) gave written informed consent.

Sixteen AD and 16 DLB patients were recruited from our Memory Clinic and Movement Disorder Clinic. Thirteen age-matched volunteers come from our nondemented case register cohorts. The diagnosis of probable AD was made using National Institute of Neurological and Communicative Diseases and Stroke/Alzheimer's Disease and Related Disorders Association criteria (McKhann et al. 1984). The probable DLB diagnosis was based on consensus guidelines (McKeith et al. 2005) with a specific restriction: we included only patients with the presence of flCog, plus at least one additional core feature (visual hallucination or parkinsonism) or the presence of flCog plus one or more suggestive features (McKeith et al. 2005).

As part of their clinical work up within 6 months before the inclusion in the study, all patients underwent computerized tomography or MRI and dopaminergic presynaptic ligand ioflupane SPECT (DAT scan). In addition all patients were assessed with electroencephalography (EEG) recordings as abnormalities characterized by parieto-occipital dominant frequency alterations have previously been shown to reliably differentiate probable DLB from AD (Bonanni et al. 2008). DAT scans and EEG Compressed Spectral Array patterns (as defined in Bonanni et al. 2008), performed prior to entry into the study, were used to support the diagnosis of DLB.

Clinical Evaluation

Mini mental state examination (MMSE), clinical dementia rating (CDR) and Dementia rating scale-2 (DRS-2) (Jurica et al. 2001) were performed for global cognitive assessment. Frontal assessment battery (FAB) was performed to evaluate the severity of frontal dysfunction (Dubois et al. 2000). The frequency and duration of flCog were assessed by CAF questionnaire (Walker et al. 2000); this is a well established tool and while it has been superseded by scales which may have better diagnostic utility in distinguishing flCog in DLB compared with AD (e.g., dementia cognitive fluctuation scale, Lee et al. 2013), the CAF remains validated as a measure of the severity and frequency of flCog and has been used in numerous studies as a metric to examine the pathophysiological basis of flCog (Ballard, O'Brien et al. 2001; Ballard, Walker et al. 2001b; Bonanni et al. 2008; Taylor et al. 2013; Peraza et al. 2014). A CAF score between 2 and 16 was considered sufficient to define a patient as affected by flCog (Bonanni et al. 2008). Based on this criterion only a 2% of our DLB selected population was excluded from the study. AD patients were selected on the basis of having no clinical history of flCog (CAF score of zero). Extrapyramidal signs were assessed using the motor part of the Unified Parkinson's Disease Rating Scale (UPDRS) III (Fahn and Elton 1987). The Neuropsychiatric Inventory (NPI) scale was used to evaluate neuropsychiatric features (Cummings et al. 1994). The NPI hallucinations item-2 scale was performed to investigate the occurrence and severity of visual hallucinations. Minimal International Classification of Sleep Disorders criteria were used to assess REM sleep behavior disorder (RBD) (World Health Organization 1992). Since ^{1}H-MRS spectra are sensitive to pharmacological manipulations (Gomez et al. 2012; Stone et al. 2012; Karczewska-Kupczewska et al. 2013), pharmacological treatments were withdrawn on the day of MR session (Onofrj et al. 2003; Burn et al. 2006; Franciotti et al. 2013).

MR Protocol

All MR data were acquired with a Philips Achieva 3 T scanner (Philips Medical System, Best, the Netherlands) equipped with 8-channel receiver coil. Three-dimensional T_1-weighted images were acquired by using Turbo Field-Echo sequence (TFE, TR/TE = 11/5 ms, slice thickness of 0.8 mm). Two ^{1}H-MRS voxels of 1.5 × 1.0 × 1.5 mm^3 were accurately placed on right and left thalami, respectively (Fig. 1*A*). Point-resolved spectroscopy sequences (TR/TE = 2000/39 ms, 16-step phase-cycle and an average of 128 scan) with and without water suppression were performed by using chemically shift selective (CHESS) pulses. One thousand and twenty-four points were acquired with a spectral width of 2000 Hz. T_2-weighted fluid attenuation inversion recovery sequence [FLAIR, time repetition (TR)/time echo (TE) = 11 000/125 ms, slice thickness of 4 mm, field of view (FOV) = 240 × 129 × 222 mm] was performed to exclude participants with concomitant vascular pathology or with white matter abnormalities outside the normal range.

^{1}H-MRS Analysis

^{1}H-MRS data analysis was performed by using JMRUI version 4.0 (Naressi et al. 2001). Spectra with water suppression were filtered for removal of residual water by using the Hankel Lanczos Singular Values Decomposition algorithm. After autophasing, baseline and frequency shifts correction, a priori knowledge database (NAA, 2.02 ppm; total creatine = tCr, 3.03 ppm; tCho, 3.22 ppm) was created to put constraints on the advanced magnetic resonance fitting algorithm within jMRUI package. Peak shifts were restricted to ±5 ppm of the theoretical location. Spectra with artifact and metabolites fits with Cramer Rao Lower Bounds >20% were excluded.

For applicability to the clinical practice and because several ^{1}H-MRS studies report stable tCr levels in dementias (Valenzuela and Sachdev 2001; Dedeoglu et al. 2004; Chao et al. 2005; Kantarci 2013), we expressed NAA and tCho relatively to tCr. By using spectra without water suppression, we calculated the area of the water peak and we used it as an internal reference standard for absolute tCr quantification (Christiansen et al. 1993; Delli Pizzi et al. 2012, 2013).

Parcellation of Thalami

Functional MRI of the Brain (FMRIB) Software Library (FSL, version 5.0; http://www.fmrib.ox.ac.uk/fsl, Smith et al. 2004) was used to perform structural connectivity-based parcellation of thalami and to investigate microstructural changes in each thalamic region. For each subject, mean diffusivity (MD) maps were generated from a tensor-model fit in FSL (FDT, FMRIB's Diffusion Toolbox). Thalami parcellation was performed according to methods described by Behrens et al. (2003). Four cortical masks including prefrontal, sensorimotor, temporal, and parieto-occipital regions were defined using the Harvard Oxford Cortical Atlas (implemented in FSL) (Fig. 2*A*). The composition of each target region was reported in Supplementary Table 1. FMRIB's Integrated Registration and Segmentation Tool (FIRST) was used to automatically segment thalami (Patenaude et al. 2011) and its outputs were binarized to obtain masks. All cortical and subcortical masks were in MNI space (1 × 1 × 1 mm). After Bayesian estimation of diffusion parameters obtained using sampling techniques, the DTI maps were registered to MNI standard space using: (1) FLIRT to register each subject's b0 image to its native structural image, and (2) FMRIB's nonlinear registration tools to register the structural and diffusion images to MNI space (1 × 1 × 1 mm). All masks were then propagated onto each individual's DTI scalar maps using the inverse of the above transformations. To exclude thalamic voxels that contained cerebrospinal fluid (CSF), the b0 images were segmented using FMRIB's Automated Segmentation Tool (FAST) and CSF binarized to be used as exclusion mask. To exclude voxels out of the thalamic range, manual editing was applied where needed. Next, probabilistic tracking was carried out by probabilistic tracking (PROBTRACKX) tool. "Find the biggest" command line was used to define the thalamic connectivity-defined subregions according to their highest probability of connection with cortical regions (Fig. 2*B*). Two experienced operators visually inspected the "find the biggest" outputs, verifying the anatomic correspondence of each thalamic connectivity-defined subregion among subjects and their accordance with Oxford Thalamic Connectivity Atlas (integrated in FSL, Johansen-Berg et al. 2005; Fig. 2*C*).

Finally, MD values were calculated in each connectivity-defined subregion.

Given that some cortical regions in DLB and/or AD could be characterized by changes in regional cerebral blood flow (Colloby et al. 2013) and the diffusion indices could be biased by different location and volume of thalamic connectivity-defined regions determined by the tracking algorithm, we adopted 3 different strategies. Firstly, we verified whether the spatial distribution and the connection probability within each thalamic connectivity-defined region were altered by the pathological underlying condition (Nair et al. 2013). Specifically, by using "randomize" command line, we carried out comparisons within and between groups on the maps of connection probability generated by PROBTRACKX (Fig. 2*D*). Family-wise error (FEW) correction was applied to obtain the significant voxels. Secondly, we verified whether the volumes of each thalamic region defined by "find the biggest" were significantly different among groups. Specifically, for each subject, the

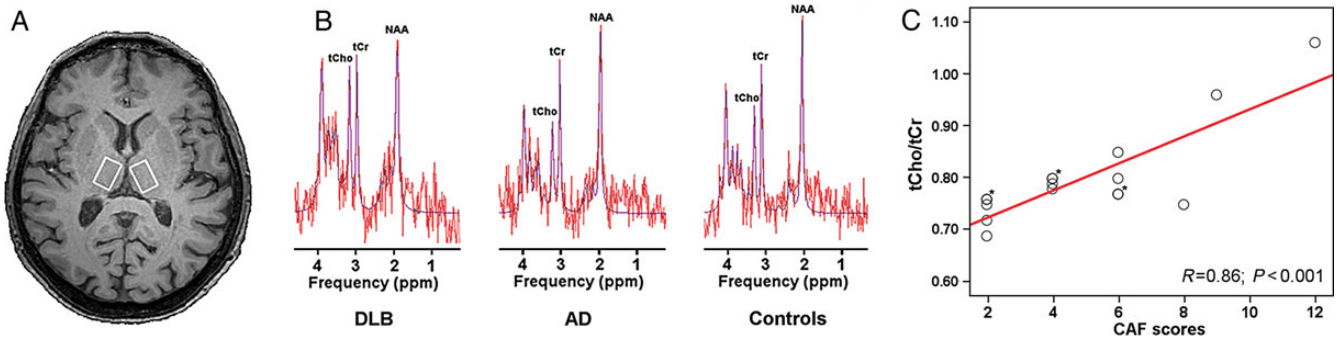

Figure 1. Proton magnetic resonance spectroscopy (^{1}H-MRS). (*A*) Two voxels of 1.5 × 1.0 × 1.5 mm^3 were, respectively, placed on right and left thalami by using T_1-weighted image as anatomical reference. (*B*) Representative spectra for DLB, AD, and controls. Estimated signals (violet) were reported on original signals (red). NAA, *N*-acetyl-aspartate (2.02 ppm); tCr, total creatine (3.03 ppm); tCho, total choline (3.22 ppm). (*C*) Scatterplot expresses the linear regression between CAF scores and tCho/tCr values in the right thalamus. AD, Alzheimer's disease; DLB, dementia with Lewy bodies. Values marked with an asterisk are overlapped.

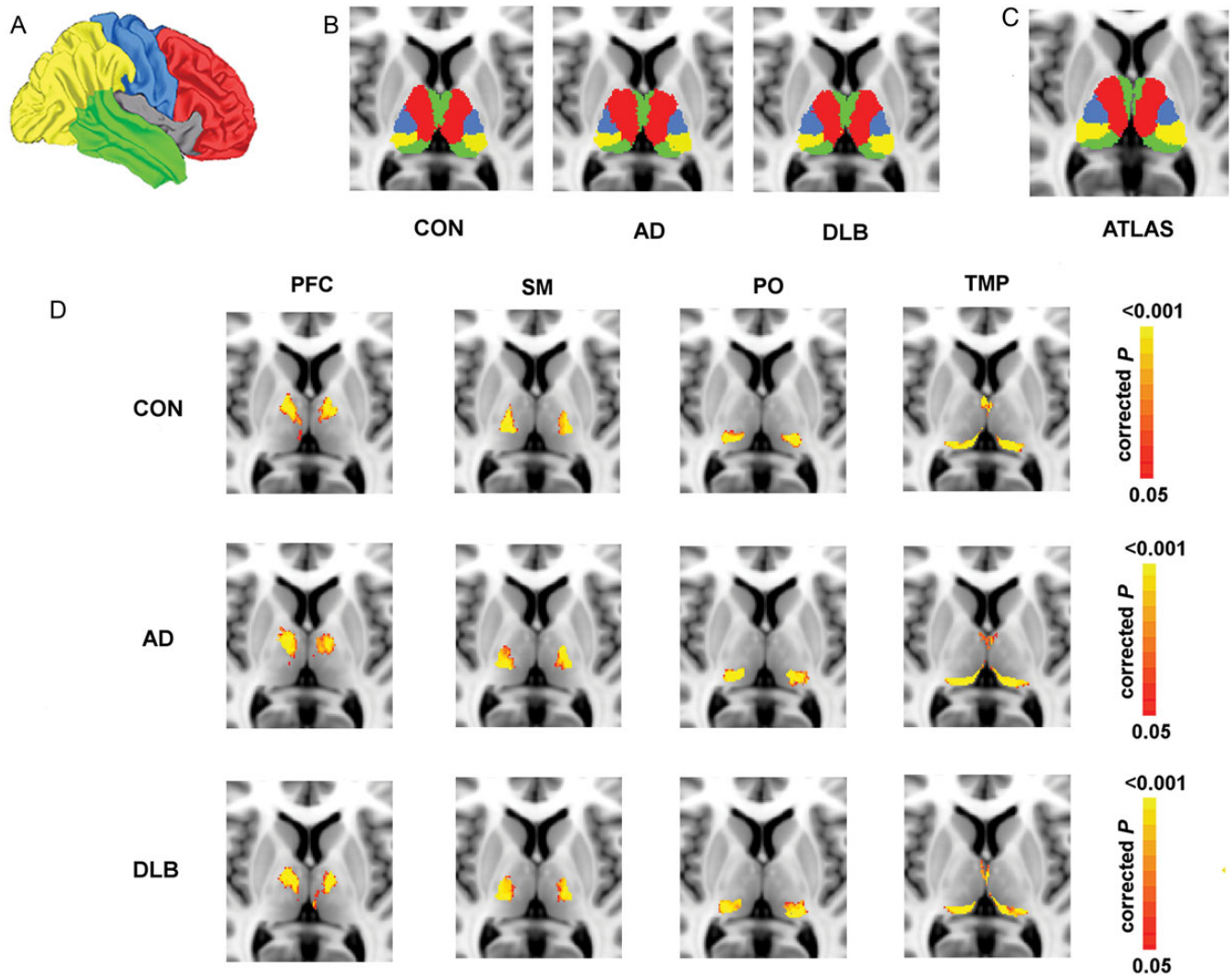

Figure 2. Structural connectivity. (*A*) Cortical rendering of target regions used for thalami parcellation (colors were in agreement with thalamic connectivity). (*B*) Connectivity-based subdivision of thalami for controls (CON), dementia with Lewy bodies (DLB), and Alzheimer's disease (AD). Thalamic voxels are classified and colored according to the highest probability of connection to specific cortical regions. Red, connectivity-defined subregion (CDR) that projects from thalamus to prefrontal cortex; blue, CDR that projects from thalamus to sensorimotor cortex; yellow, CDR that projects from thalamus to parieto-occipital cortex; green, CDR that projects from thalamus to temporal cortex. (*C*) Thalami regions defined by Oxford Thalamic Connectivity Atlas. (*D*) Within-group probabilistic tractography maps for each cortical target region. The significant results are shown by voxels rating from red to yellow ($P < 0.05$, FWE-corrected). No significant differences were found among groups. PFC, prefrontal; SM, sensorimotor; PO, parieto-occipital; TMP, temporal.

volumes of thalamic regions were calculated by "fslstats" command line and, next, they were normalized for ipsilateral thalamic volume. Third, we verified whether the MD values in each thalamic region were related to differences found by tracking probability. Specifically, we defined the thalamic regions from Oxford thalamic connectivity atlas and we extracted MD values from them. Finally, we performed multivariate analysis of variance (MANOVA) on MD values to test whether the 2 methods (probabilistic parcellation and atlas) provided different results for thalamic regions.

Statistical Analysis

Analysis of variance (ANOVA) among groups was carried out on demographic and clinical data. χ^2 test was carried out for gender.

We performed multivariate analysis of covariance (MANCOVA) to exclude the possible effect of cognitive impairment on different imaging findings obtained from demented patients and controls. Next, MANOVA was carried out to test the differences among groups (AD, DLB, and controls). Tukey's HSD post hoc test was performed for assessing pair-wise differences between groups. For all comparisons, significance level was set at $P < 0.05$.

Linear regression was performed to assess the relationship between MR outcomes in DLB patients (MD within right and left connectivity-defined subregions and metabolites/tCr within left and right thalami) and CAF scores (our primary clinical measure). Age, MMSE, NPI hallucination-item, UPDRS scores were included as nuisance factors. All results were corrected for multiple comparisons using Bonferroni's correction ($P = 0.05/12 = 0.004$).

Results

Demographic and Clinical Features

Table 1 summarizes demographic features and neuropsychological test scores. Groups did not differ for age, gender, and educational level. CAF scores ranged between 2 and 12 in DLB patients. All DLB patients showed an abnormal quantitative EEG pattern profile consistent with a DLB diagnosis (Bonanni et al. 2008) and represented by slow dominant frequency (in the theta and prealpha band) in posterior leads and a dominant frequency variability >1.5 Hz. None of the AD patients or controls showed these DLB-specific EEG characteristics (Bonanni et al. 2008). No differences on global test of cognition and on severity of frontal dysfunction were reported between AD and DLB patients. Fourteen DLB patients had RBD. Dopamine-transporter hypocaptation in the caudate nuclei at SPECT-DAT scan was observed in all DLB patients, and it was bilateral in 12 patients. SPECT-DAT scan abnormalities were not observed in AD patients or control subjects.

The patients were on a range of medications including L-Dopa (all DLB patients), rivastigmine or donepezil (all AD and DLB patients with no differences in daily dosages between the 2 groups of patients), quetiapine (8 DLB and 6 AD), clozapine (4 DLB), and risperidone (4 AD) and clonazepam (the 14 DLB patients with RBD).

Table 1
Demographic and clinical features

Characteristics	Controls	AD	DLB
Number of subjects/patients	13	16	16
Age[a,b]	75.6 ± 4.7	75.5 ± 5.4	75.6 ± 4.2
Male gender (%)[c]	46%	50%	50%
Disease duration (years)[d]	–	3.1 ± 0.7	3.0 ± 0.6
Education level (years)[a,e]	7 ± 4	7 ± 3	7 ± 4
Clinical dementia rating[a,f]	–	2.3 ± 0.6	2.3 ± 0.7
Mini mental state examination[a,g]	28.3 ± 1.3	17.7 ± 4.5	17.9 ± 4.5
Dementia rating scale[a,h]	136.6 ± 0.7	91.4 ± 18.1	91.7 ± 15.8
Frontal assessment battery[a,i]	17.6 ± 0.5	8.4 ± 2.7	8.6 ± 2.7
Clinician assessment of fluctuations	0.0 ± 0.0	0.0 ± 0.0	4.9 ± 2.9
Unified Parkinson's disease rating scale III	0.0 ± 0.0	0.0 ± 0.0	25.8 ± 10.0
Neuropsychiatric inventory-item 2 hallucinations	0.0 ± 0.0	0.0 ± 0.0	4.0 ± 1.8

Note: Values are expressed as mean ± standard deviation.
[a]The *P*-values were calculated using the one-way ANOVA; Tukey"s HSD post hoc test was also performed when *F*-test was significant.
[b]Main interaction among groups: $F_{2,44} = 0.003$, $P = 0.997$.
[c]The *P*-values were calculated using χ^2 test: $\chi^2_1 = 0.022$, $P = 0.881$.
[d]The *P*-values were calculated using the independent-samples *t*-test: $t_{30} = -0.522$, $P = 0.605$.
[e]Main interaction among groups: $F_{2,44} = 0.846$, $P = 0.436$.
[f]The *P*-values were calculated using the independent-samples *t*-test: $t_{30} = -0.275$; $P = 0.786$.
[g]Main interaction among groups: $F_{2,44} = 34.223$, $P < 0.001$; post hoc: controls versus AD, $P < 0.001$; controls versus DLB, $P < 0.001$ and AD versus DLB, $P = 0.982$.
[h]Main interaction among groups: $F_{2,44} = 45.367$, $P < 0.001$; post hoc: controls versus AD, $P < 0.001$; controls versus DLB, $P < 0.001$ and AD versus DLB, $P = 0.998$.
[i]Main interaction among groups: $F_{2,44} = 74.363$, $P < 0.001$; post hoc: controls versus AD, $P < 0.001$; controls versus DLB, $P < 0.001$ and AD versus DLB, $P = 0.987$.

^{1}H-MRS Findings

Table 2 summarizes ^{1}H-MRS results. Figure 1*B* shows representative spectra for each group. Supplementary Table 2 shows the effects among groups from MANCOVA and MANOVA analyses. Lower NAA/tCr and higher tCho/tCr values were bilaterally observed in the thalami of DLB patients respect to controls. No changes were found in the thalami of AD patients compared with controls. The comparison between DLB and AD demonstrated tCho/tCr increase in the right thalamus of DLB patients. No tCr changes were found among groups. Assuming as nuisance factors age, MMSE, NPI hallucinations, UPDRS scores, on linear regression a significant relationship between tCho/tCr and CAF values within right thalamus ($R = 0.86$, $t = 5.391$, $P < 0.001$) (Fig. 1*C*) was observed.

Thalamocortical Structural Connectivity

Figure 2*B* shows the thalamic connectivity-defined subregions projecting to:

1. prefrontal cortex including the ventro-anterior and dorso-medial parts of the thalami;
2. sensorimotor cortex including the ventrolateral part of the thalami;
3. parieto-occipital cortex including the ventro-posterior part of the thalami and the superior portion of pulvinar;
4. temporal cortex including the dorso-anterior part of the thalami and the inferior portion of pulvinar.

Figure 2*D* shows the maps of connection probability of each thalamic subregion to specific cortical regions, for each group. When comparisons between groups were performed, no significant differences were observed on connection probability. As verified by visual inspection of "find the biggest" outputs, the location of each connectivity-defined thalamic region showed good correspondence among groups and it was in agreement with Oxford Thalamic Connectivity Atlas (Fig. 2*C*). Furthermore, the volumes of each thalamic region defined by "find the biggest" were not different among groups (see Supplementary Table 3). Hence, the anatomy for each thalamic connectivity-defined region did not significantly change in pathological conditions with respect to controls.

Mean Diffusivity Changes Within Thalamic Regions

Table 3 shows grand mean MD values for each connectivity-defined subregion obtained from tractography-based subdivision

Table 2
Neurochemical changes in the thalami assessed by ^{1}H-MRS

Metabolites	Thalamus	Controls	AD	DLB	AD versus controls[a]	DLB versus controls[a]	AD versus DLB[a]
NAA/tCr	Right	1.84 ± 0.12	1.73 ± 0.15	1.65 ± 0.2	$P = 0.160$	P **= 0.008**	$P = 0.363$
	Left	1.82 ± 0.15	1.78 ± 0.19	1.68 ± 0.14	$P = 0.738$	P **= 0.045**	$P = 0.173$
tCho/tCr	Right	0.72 ± 0.04	0.72 ± 0.07	0.8 ± 0.09	$P = 0.996$	P **= 0.014**	P **= 0.011**
	Left	0.72 ± 0.05	0.76 ± 0.08	0.8 ± 0.11	$P = 0.315$	P **= 0.034**	$P = 0.465$
tCr/water[b]	Right	5.2 ± 0.2	5.1 ± 0.4	4.9 ± 0.9	$P = 0.958$	$P = 0.414$	$P = 0.546$
	Left	5.2 ± 0.6	5.0 ± 0.7	5.0 ± 0.7	$P = 0.733$	$P = 0.774$	$P = 0.997$

AD, Alzheimer's disease; DLB, dementia with Lewy bodies; NAA, *N*-acetyl-aspartate; tCr, total creatine; tCho, total choline.
[a]Tukey's HSD post hoc test was performed for assessing pair-wise differences between groups.
[b]Value $\times 10^{-4}$. Bold characters indicate statistically significant results. Significant mean differences were found among groups by MANOVA ($F_{12,74} = 3.216$, $P = 0.001$).

Table 3
Mean diffusivity values in each "connectivity-defined region" obtained from tractography-based parcellation of thalami

Connectivity-defined region		Mean diffusivity (MD)			Statistical comparison[a]		
Target	Thalamus	Controls	AD	DLB	AD versus controls	DLB versus controls	AD versus DLB
Prefrontal cortex	Right	752 ± 15	785 ± 67	809 ± 52	$P = 0.211$	P **= 0.014**	$P = 0.395$
	Left	752 ± 16	784 ± 72	815 ± 52	$P = 0.257$	P **= 0.008**	$P = 0.243$
Sensorimotor cortex	Right	750 ± 19	757 ± 71	797 ± 60	$P = 0.933$	$P = 0.079$	$P = 0.131$
	Left	750 ± 37	760 ± 80	801 ± 47	$P = 0.876$	$P = 0.061$	$P = 0.136$
Parieto-occipital cortex	Right	759 ± 24	793 ± 88	843 ± 61	$P = 0.365$	P **= 0.004**	$P = 0.085$
	Left	759 ± 28	798 ± 93	837 ± 59	$P = 0.289$	P **= 0.010**	$P = 0.234$
Temporal cortex	Right	779 ± 20	828 ± 70	818 ± 52	P **= 0.046**	$P = 0.134$	$P = 0.856$
	Left	782 ± 24	830 ± 59	818 ± 47	P **= 0.024**	$P = 0.111$	$P = 0.757$

Note: MD values ($\times 10^{-4}$mm^2/s) are expressed as mean ± standard deviation. Bold characters indicate statistically significant results. Significant mean differences were found among groups by MANOVA ($F_{16,70} = 3.124$, $P = 0.001$).
[a]*P*-values from Tukey's HSD post hoc.
AD, Alzheimer's disease; DLB, dementia with Lewy bodies.

of thalami. Supplementary Table 4 shows the effects among groups from MANCOVA and MANOVA analyses. Supplementary Table 5 shows grand mean MD values for each connectivity-defined subregion obtained from Oxford thalamic connectivity atlas. No differences were found between MD values obtained with probabilistic parcellation and MD values obtained with Oxford Thalamic Connectivity Atlas (see Supplementary Table 6).

In comparison to controls, DLB patients showed bilateral increases in MD in the connectivity-defined subregions projecting to the prefrontal and parieto-occipital cortices. As compared with controls, AD patients showed increase of MD in left connectivity-defined subregion projecting to the temporal cortex. No significant differences were found in the comparison between DLB and AD. Within the DLB group MD increases were not correlated with our primary measure of flCog (CAF score) or other clinical variables (e.g. FAB).

Discussion

In the current study, we demonstrated that DLB patients with flCog were affected by neurochemical imbalance in the thalami and by microstructural changes in the connectivity-defined regions projecting from thalamus to the frontal and parieto-occipital cortices.

Specifically, we found reduced NAA/tCr and increased tCho/tCr in the thalami of DLB with flCog.

TCr is a neuronal marker of energetic metabolism. Because its levels are typically stable in dementias (Kantarci 2013), tCr has been used as internal reference in ^{1}H-MRS studies on DLB (Molina et al. 2002; Kantarci et al. 2004; Graff-Radford et al. 2014). Consistent with this, our results showed that tCr was effectively unchanged in our groups, and thus suggest that the thalamic neurochemical alterations observed in our DLB patients are mainly attributable to NAA and tCho.

NAA is primarily located in neuron bodies, axons, and dendrites and it is a sensitive marker for neuronal density or viability (Kantarci 2013). Therefore, NAA reduction suggested that DLB pathology could be associated to neurodegenerative processes in the thalami. Notably, this finding is consistent with a recent DTI study describing thalamic white matter disruption in DLB patients (Watson et al. 2012).

TCho provides a marker of the contribution of cytosolic glycerolphosphocholine and phosphocholine which are the products of membrane phosphatidyl choline breakdown and the precursors of choline and acetylcholine synthesis, respectively (Klein 2000). It was hypothesized that higher tCho levels in DLB could be linked to the increase of membrane turnover due to dying of the neuropil and to down-regulation of choline acetyltransferase activity that it is reduced more severely in DLB with respect to AD (Wurtman et al. 1985; MacKay et al. 1996; Tiraboschi et al. 2002; Kantarci 2013). In this context, recent ^{1}H-MRS studies have suggested that the increase in tCho could be a characteristic feature of DLB and independent from AD pathology (Kantarci 2013; Graff-Radford et al. 2014). Furthermore, consistently with our findings on thalami, Kotagal et al. (2012) observed thalamic cholinergic denervation in DLB but not in AD, suggesting a relationship between neurodegenerative involvement of thalamic cholinergic afferent projections and cognitive alteration in DLB.

TCho/tCr values in the thalamus were closely correlated with the presence and severity of flCog as assessed by CAF questionnaire. The cholinergic system is particularly implicated in attention and awareness (Perry et al. 1999; Klinkenberg et al. 2011). Studies on DLB patients reported attentional performance improvement following the cholinesterase inhibitors treatment (Wesnes et al. 2005). Furthermore, imaging studies observed

cholinergic alterations related to flCog in the thalami of DLB patients (Perry et al. 1998; O'Brien et al. 2005; Pimlott et al. 2006). Thus, this strongly favors the role of cholinergic imbalance within thalami in the etiology of flCog in DLB.

In agreement with previous functional and structural studies by our groups (Franciotti et al. 2006, 2013; Delli Pizzi et al. 2014), we also observed predominant right lateralization of neurochemical alterations in DLB. These findings could be linked to the dominant role of the right hemisphere in attention (Thiebaut de Schotten et al. 2011). Further studies integrating structural and functional MRI techniques could clarify whether predominant right hemispheric dysfunction is truly a specific feature of DLB.

We observed that structural thalamocortical connectivity was affected in DLB patients with flCog. In this context, MD was specifically assessed because it is an index for both grey and white matters damage and its high values are associated to reduction in membrane density and cell loss of both neurons and glia (Canu et al. 2010).

Thalamic neurons regulate the cortico-cortical control acting as neuronal hub to synchronize oscillations between cortical areas (Sherman 2007). The modulation of thalamic activity can shift cortical activity by desynchronizing activated states (depolarized tonic firing mode) associated with arousal and/or by synchronizing deactivated states (burst firing mode) indicative of drowsiness (Llinás and Steriade 2006; Hirata and Castro-Alamancos 2010). In this context, impaired thalamic activity has been associated with decreased levels of arousal (Volkow et al. 1995; Fiset et al. 1999).

We found that MD was bilaterally increased in the connectivity-defined subregion projecting from thalamus to frontal cortex in DLB as compared with controls. The thalamic nuclei serving prefrontal cortex play a relevant role in consciousness (Foucher et al. 2004; Ward 2011) and alertness (Tomasi et al. 2009). In particular, deficits in concentration can be observed when thalamic region projecting to prefrontal cortical network is damaged (Van Der Werf et al. 1999). Moreover, in agreement with our findings, a recent study showed that functional connectivity within thalamic region projecting to frontal lobe was altered in DLB patients with respect to controls (Kenny et al. 2013). However, we did not observe a significant relationship between MD and CAF or FAB scores. However, in some respects this is not unexpected as across different neuroimaging modalities there has been an emphasis on symptom in DLB being more reliant upon posterior cortical function (Imamura et al. 1999; Lobotesis et al. 2001; Pasquier et al. 2002; Kemp et al. 2007; Taylor et al. 2012; Delli Pizzi et al. 2014). Indeed, in support of this we found that MD was bilaterally increased in the connectivity-defined subregion projecting from thalamus to parieto-occipital cortex in DLB as compared with controls although again there was no relationship between MD and CAF for these projections. Therefore, while the integrity of thalamocortical projections may be disrupted in DLB, this may be less relevant to the pathophysiology of flCog; the ^{1}H-MRS findings noted above support an argument that intrinsic neurochemical changes in the thalamus are more important, at least for flCog.

The ventrolateral region of thalamus and anterior portion of pulvinar synchronize the activity across posterior cortical regions, filtering distracters (Fischer and Whitney 2012) and regulating visuospatial attention (Saalmann et al. 2012). Particularly, pulvinar is ideally situated to integrate bottom-up orienting, driven either by sensory and subcortical inputs, with top-down orienting, driven by goals and context (Ward 2011). Notably, it was observed close relationship between pulvinar lesion and visuo-attentional deficits (Arend et al. 2008). On these bases, we propose that the deregulation of parieto-occipito-thalamic connectivity could be related to alteration in visual attention and visual dysfunction characterizing DLB patients.

Furthermore, we observed that AD patients were affected by bilateral microstructural damage in the connectivity-defined subregion projecting from thalamus to temporal cortex. As assessed by structural connectivity analysis, this connectivity-defined subregion included the antero-ventral nuclei of thalamus and the posterior pulvinar nuclei, which are directly connected to hippocampus via the fornix and via the temporo-pulvinar tract. The integrity of these connections is essential for episodic memory (Aggleton and Brown 1999), which is specifically affected in AD (Di Paola et al. 2007). In this context, Zarei et al. (2010) reported that AD patients were affected by structural alteration of the antero-dorsal thalamic nuclei. Therefore, we suggest that the microstructural alteration of connectivity-defined subregion projecting from thalamus to temporal cortex could be linked to great memory impairment affecting AD patients.

In conclusion, our findings highlight the critical role of thalamus in DLB pathology. By multimodal techniques including structural MRI, DTI, and ^{1}H-MRS, we have shown, firstly, microstructural damage in thalamic regions related to alertness and attention and, secondly, metabolic alterations related to neuronal damage and cholinergic dysfunction in the thalami. Furthermore, our results suggest that cholinergic imbalance within thalami is closely linked to frequency and duration of flCog occurring in DLB.

A possible limitation of our study is that we focused our analyses on DLB patients with flCog. Therefore our conclusions may be less applicable to DLB without flCog. However, we underline that in the present study a CAF score $\geq$2 was considered sufficient to define a patient as affected by flCog (Bonanni et al. 2008), at difference with the study in which this scale was originally proposed, where a higher cut-off of 5 at the CAF questionnaire was shown to have high sensitivity and specificity to DLB.

Supplementary Material

Supplementary material can be found at: http://www.cercor.oxfordjournals.org/.

Funding

Funding to pay the Open Access publication charges for this article was provided by Wellcome Trust.

Notes

Conflict of Interest: None declared.

References

Aggleton JP, Brown MW. 1999. Episodic memory, amnesia, and the hippocampal-anterior thalamic axis. Behav Brain Sci. 22:425–489.

Arend I, Rafal R, Ward R. 2008. Spatial and temporal deficits are regionally dissociable in patients with pulvinar lesions. Brain. 131:2140–2152.

Ballard C, O'Brien J, Gray A, Cormack F, Ayre G, Rowan E, Thompson P, Bucks R, McKeith I, Walker M et al. 2001. Attention and fluctuating attention in patients with dementia with Lewy bodies and Alzheimer disease. Arch Neurol. 58:977–982.

Ballard C, Walker M, O'Brien J, Rowan E, McKeith I. 2001. The characterisation and impact of 'fluctuating' cognition in dementia with Lewy bodies and Alzheimer's disease. Int J Geriatr Psychiatry. 16:494–498.

Behrens TE, Johansen-Berg H, Woolrich MW, Smith SM, Wheeler-Kingshott CA, Boulby PA, Barker GJ, Sillery EL, Sheehan K, Ciccarelli O et al. 2003. Non-invasive mapping of connections between human thalamus and cortex using diffusion imaging. Nat Neurosci. 6:750–757.

Bonanni L, Thomas A, Tiraboschi P, Perfetti B, Varanese S, Onofrj M. 2008. EEG comparisons in early Alzheimer's disease, dementia with Lewy bodies and Parkinson's disease with dementia patients with a 2-year follow-up. Brain. 131:690–705.

Burn D, Emre M, McKeith I, De Deyn PP, Aarsland D, Hsu C, Lane R. 2006. Effects of rivastigmine in patients with and without visual hallucinations in dementia associated with Parkinson's disease. Mov Disord. 21:1899–1907.

Canu E, McLaren DG, Fitzgerald ME, Bendlin BB, Zoccatelli G, Alessandrini F, Pizzini FB, Ricciardi GK, Beltramello A, Johnson SC et al. 2010. Micro-structural diffusion changes are independent of macrostructural volume loss in moderate to severe Alzheimer's disease. J Alzheimers Dis. 19:963–976.

Chao LL, Schuff N, Kramer JH, Du AT, Capizzano AA, O'Neill J, Wolkowitz OM, Jagust WJ, Chui HC, Miller BL et al. 2005. Reduced medial temporal lobe N-acetylaspartate in cognitively impaired but nondemented patients. Neurology. 64:282–289.

Christiansen P, Henriksen O, Stubgaard M, Gideon P, Larsson HB. 1993. In vivo quantification of brain metabolites by 1H-MRS using water as an internal standard. Magn Reson Imaging. 11:107–118.

Colloby SJ, Taylor JP, Davison CM, Lloyd JJ, Firbank MJ, McKeith IG, O'Brien JT. 2013. Multivariate spatial covariance analysis of 99mTc-exametazime SPECT images in dementia with Lewy bodies and Alzheimer's disease: utility in differential diagnosis. J Cereb Blood Flow Metab. 33:612–618.

Cummings JL, Mega M, Gray K, Rosenberg-Thompson S, Carusi DA, Gornbein J. 1994. The neuropsychiatric inventory: comprehensive assessment of psychopathology in dementia. Neurology. 44: 2308–2314.

Dedeoglu A, Choi JK, Cormier K, Kowall NW, Jenkins BG. 2004. Magnetic resonance spectroscopic analysis of Alzheimer's disease mouse brain that express mutant human APP shows altered neurochemical profile. Brain Res. 1012:60–65.

Delli Pizzi S, Madonna R, Caulo M, Romani GL, De Caterina R, Tartaro A. 2012. MR angiography, MR imaging and proton MR spectroscopy in-vivo assessment of skeletal muscle ischemia in diabetic rats. PLoS One. 7:e44752.

Delli Pizzi S, Rossi C, Di Matteo V, Esposito E, Guarnieri S, Mariggiò MA, Franciotti R, Caulo M, Thomas A, Onofrj M et al. 2013. Morphological and metabolic changes in the nigro-striatal pathway of synthetic proteasome inhibitor (PSI)-treated rats: a MRI and MRS study. PLoS One. 8:e56501.

Delli Pizzi S, Rossi C, Di Matteo V, Esposito E, Guarnieri S, Mariggiò MA, Franciotti R, Caulo M, Thomas A, Onofrj M et al. 2014. Structural Alteration of the dorsal visual network in DLB patients with visual hallucinations: a cortical thickness MRI study. PLoS ONE. 9:e86624.

Di Paola M, Macaluso E, Carlesimo GA, Tomaiuolo F, Worsley KJ, Fadda L, Caltagirone C. 2007. Episodic memory impairment in patients with Alzheimer's disease is correlated with entorhinal cortex atrophy. A voxel-based morphometry study. J Neurol. 254:774–781.

Dubois B, Slachevsky A, Litvan I, Pillon B. 2000. The FAB: a frontal assessment battery at bedside. Neurology. 55:1621–1626.

Fahn S, Elton RL. 1987. Members of the Unified Parkinson's Disease Rating Scale Development Committee. Unified Parkinson's disease rating scale. In: Fahn S et al. editors. Recent development in Parkinson's disease. Florham Park (NJ): Macmillan Healthcare Information. p. 153–164.

Fischer J, Whitney D. 2012. Attention gates visual coding in the human pulvinar. Nat Commun. 3:1051.

Fiset P, Paus T, Daloze T, Plourde G, Meuret P, Bonhomme V, Hajj-Ali N, Backman S, Evans A. 1999. Brain mechanisms of propofol-induced loss of consciousness in humans: a positron emission tomographic study. J Neurosci. 19:5506–5513.

Foucher JR, Otzenberger H, Gounot D. 2004. Where arousal meets attention: a simultaneous fMRI and EEG recording study. Neuroimage. 22:688–697.

Franciotti R, Falasca NW, Bonanni L, Anzellotti F, Maruotti V, Comani S, Thomas A, Tartaro A, Taylor JP, Onofrj M. 2013. Default network is not hypoactive in dementia with fluctuating cognition: an Alzheimer disease/dementia with Lewy bodies comparison. Neurobiol Aging. 34:1148–1158.

Franciotti R, Iacono D, Della Penna S, Pizzella V, Torquati K, Onofrj M, Romani GL. 2006. Cortical rhythms reactivity in AD, LBD and normal subjects: a quantitative MEG study. Neurobiol Aging. 27:1100–1109.

Graff-Radford J, Boeve BF, Murray ME, Ferman TJ, Tosakulwong N, Lesnick TG, Maroney-Smith M, Senjem ML, Gunter J, Smith GE et al. 2014. Regional proton magnetic resonance spectroscopy patterns in dementia with Lewy bodies. Neurobiol Aging. 35:1483–1490.

Gomez R, Behar KL, Watzl J, Weinzimer SA, Gulanski B, Sanacora G, Koretski J, Guidone E, Jiang L, Petrakis IL et al. 2012. Intravenous ethanol infusion decreases human cortical γ-aminobutyric acid and N-acetylaspartate as measured with proton magnetic resonance spectroscopy at 4 tesla. Biol Psychiatry. 71:239–246.

Hirata A, Castro-Alamancos MA. 2010. Neocortex network activation and deactivation states controlled by the thalamus. J Neurophysiol. 103:1147–1157.

Imamura T, Ishii K, Hirono N, Hashimoto M, Tanimukai S, Kazuai H, Hanihara T, Sasaki M, Mori E. 1999. Visual hallucinations and regional cerebral metabolism in dementia with Lewy bodies (DLB). NeuroReport. 10:1903–1907.

Johansen-Berg H, Behrens TE, Sillery E, Ciccarelli O, Thompson AJ, Smith SM, Matthews PM. 2005. Functional-anatomical validation and individual variation of diffusion tractography-based segmentation of the human thalamus. Cereb Cortex. 15:31–39.

Jurica PJ, Leitten CL, Mattis S, editors. 2001. DRS-2 Dementia rating scale 2. Psychological Assessment Resources Eds. Odessa: FI.

Kantarci K. 2013. Proton MRS in mild cognitive impairment. J Magn Reson Imaging. 37:770–777.

Kantarci K, Petersen RC, Boeve BF, Knopman DS, Tang-Wai DF, O'Brien PC, Weigand SD, Edland SD, Smith GE, Ivnik RJ Jr et al. 2004. 1H MR spectroscopy in common dementias. Neurology. 63:1393–1398.

Karczewska-Kupczewska M, Tarasów E, Nikolajuk A, Stefanowicz M, Matulewicz N, Otziomek E, Górska M, Straczkowski M, Kowalska I. 2013. The effect of insulin infusion on the metabolites in cerebral tissues assessed with proton magnetic resonance spectroscopy in young healthy subjects with high and low insulin sensitivity. Diab Care. 36:2787–2793.

Kemp PM, Hoffmann SA, Tossici-Bolt L, Fleming JS, Holmes C. 2007. Limitations of the HMPAO SPECT appearances of occipital lobe perfusion in the differential diagnosis of dementia with Lewy bodies. Nucl Med Commun. 28:451–456.

Kenny ER, O'Brien JT, Firbank MJ, Blamire AM. 2013. Subcortical connectivity in dementia with Lewy bodies and Alzheimer's disease. Br J Psychiatry. 203:209–214.

Klein J. 2000. Membrane breakdown in acute and chronic neurodegeneration: focus on choline-containing phospholipids. J Neural Transm. 107:1027–1063.

Klinkenberg I, Sambeth A, Blokland A. 2011. Acetylcholine and attention. Behav Brain Res. 221:430–442.

Kotagal V, Müller ML, Kaufer DI, Koeppe RA, Bohnen NI. 2012. Thalamic cholinergic innervation is spared in Alzheimer disease compared to parkinsonian disorders. Neurosci Lett. 514:169–172.

Lee DR, McKeith I, Mosimann U, Ghosh-Nodial A, Grayson L, Wilson B, Thomas AJ. 2013. The Dementia Cognitive Fluctuation Scale, a New Psychometric Test for Clinicians to Identify Cognitive Fluctuations in People with Dementia. Am J Geriatr Psychiatry. 22:926–935.

Lee DR, Taylor JP, Thomas AJ. 2012. Assessment of cognitive fluctuation in dementia: a systematic review of the literature. Int J Geriatr Psychiatry. 27:989–998.

Llinás RR, Steriade M. 2006. Bursting of thalamic neurons and states of vigilance. J Neurophysiol. 95:3297–3308.

Lobotesis K, Fenwick JD, Phipps A, Ryman A, Swann A, Ballard C, McKeith IG, O'Brien JT. 2001. Occipital hypoperfusion on

SPECT in dementia with Lewy bodies but not AD. Neurology. 56: 643–649.
MacKay S, Ezekiel F, Di Sclafani V, Meyerhoff DJ, Gerson J, Norman D, Fein G, Weiner MW. 1996. Alzheimer disease and subcortical ischemic vascular dementia: evaluation by combining MR imaging segmentation and H-1 MR spectroscopic imaging. Radiology. 198:537–545.
McKeith I, Del Ser T, Spano P, Emre M, Wesnes K, Anand R, Cicin-Sain A, Ferrara R, Spiegel R. 2000. Efficacy of rivastigmine in dementia with Lewy bodies: a randomised, double-blind, placebo-controlled international study. Lancet. 356:2031–2036.
McKeith IG, Dickson DW, Lowe J, Emre M, O'Brien JT, Feldman H, Cummings J, Duda JE, Lippa C, Perry EK et al. Consortium on DLB. 2005. Diagnosis and management of dementia with Lewy bodies: third report of the DLB Consortium. Neurology. 65:1863–1872.
McKhann G, Drachman D, Folstein M, Katzman R, Price D, Stadlan EM. 1984. Clinical diagnosis of Alzheimer's disease: report of the NINCDS-ADRDA Work Group under the auspices of Department of Health and Human Services Task Force on Alzheimer's Disease. Neurology. 34:939–944.
Molina JA, García-Segura JM, Benito-León J, Gómez-Escalonilla C, del Ser T, Martínez V, Viaño J. 2002. Proton magnetic resonance spectroscopy in dementia with Lewy bodies. Eur Neurol. 48:158–163.
Nair A, Treiber JM, Shukla DK, Shih P, Müller RA. 2013. Impaired thalamocortical connectivity in autism spectrum disorder: a study of functional and anatomical connectivity. Brain. 136:1942–1955.
Naressi A, Couturier C, Devos JM, Janssen M, Mangeat C, de Beer R, Graveron-Demilly D. 2001. Java-based graphical user interface for the MRUI quantitation package. Magma. 12:141–152.
O'Brien JT, Firbank MJ, Mosimann UP, Burn DJ, McKeith IG. 2005. Change in perfusion, hallucinations and fluctuations in consciousness in dementia with Lewy bodies. Psychiatry Res. 139:79–88.
Onofrj M, Thomas A, Iacono D, Luciano AL, Di Iorio A. 2003. The effects of a cholinesterase inhibitor are prominent in patients with fluctuating cognition: a part 3 study of the main mechanism of cholinesterase inhibitors in dementia. Clin Neuropharmacol. 26:239–251.
Pasquier J, Michel BF, Brenot-Rossi I, Hassan-Sebbag N, Sauvan R, Gastaut JL. 2002. Value of (99 m)Tc-ECD SPET for the diagnosis of dementia with Lewy bodies. Eur J Nucl Med Mol Imaging. 29:1342–1348.
Patenaude B, Smith SM, Kennedy DN, Jenkinson M. 2011. A Bayesian model of shape and appearance for subcortical brain segmentation. Neuroimage. 56:907–922.
Peraza LR, Kaiser M, Firbank M, Graziadio S, Bonanni L, Onofrj M, Colloby SJ, Blamire A, O'Brien JT, Taylor JP. 2014. fMRI resting state networks and their association with cognitive fluctuations in dementia with Lewy bodies. Neuroimage Clin. 4:558–565.
Perry E, Court J, Goodchild R, Griffiths M, Jaros E, Johnson M, Lloyd S, Piggott M, Spurden D, Ballard C et al. 1998. Clinical neurochemistry: developments in dementia research based on brain bank material. J Neural Transm. 105:915–933.
Perry E, Walker M, Grace J, Perry R. 1999. Acetylcholine in mind: a neurotransmitter correlate of consciousness? Trends Neurosci. 22:273–280.
Piggott MA, Ballard CG, Dickinson HO, McKeith IG, Perry RH, Perry EK. 2007. Thalamic D2 receptors in dementia with Lewy bodies, Parkinson's disease, and Parkinson's disease dementia. Int J Neuropsychopharmacol. 10:231–234.
Pimlott SL, Piggott M, Ballard C, McKeith I, Perry R, Kometa S, Owens J, Wyper D, Perry E. 2006. Thalamic nicotinic receptors implicated in disturbed consciousness in dementia with Lewy bodies. Neurobiol Dis. 21:50–56.
Saalmann YB, Pinsk MA, Wang L, Li X, Kastner S. 2012. The pulvinar regulates information transmission between cortical areas based on attention demands. Science. 337:753–756.
Schiff ND. 2008. Central thalamic contributions to arousal regulation and neurological disorders of consciousness. Ann N Y Acad Sci. 1129:105–118.
Sherman SM. 2007. The thalamus is more than just a relay. Curr Opin Neurobiol. 17:417–422.
Smith SM, Jenkinson M, Woolrich MW, Beckmann CF, Behrens TE, Johansen-Berg H, Bannister PR, De Luca M, Drobnjak I, Flitney DE et al. 2004. Advances in functional and structural MR image analysis and implementation as FSL. Neuroimage. 23(Suppl 1):S208–S219.
Steriade M. 2006. Grouping of brain rhythms in corticothalamic systems. Neuroscience. 137:1087–1106.
Stone JM, Dietrich C, Edden R, Mehta MA, De Simoni S, Reed LJ, Krystal JH, Nutt D, Barker GJ. 2012. Ketamine effects on brain GABA and glutamate levels with 1H-MRS: relationship to ketamine-induced psychopathology. Mol Psychiatry. 17:664–665.
Taylor JP, Colloby SJ, McKeith IG, O'Brien JT. 2013. Covariant perfusion patterns provide clues to the origin of cognitive fluctuations and attentional dysfunction in Dementia with Lewy bodies. Int Psychogeriatr. 23:1–12.
Thiebaut de Schotten M, Dell'Acqua F, Forkel SJ, Simmons A, Vergani F, Murphy DG, Catani M. 2011. A lateralized brain network for visuospatial attention. Nat Neurosci. 14:1245–1246.
Tiraboschi P, Hansen LA, Alford M, Merdes A, Masliah E, Thal LJ, Corey-Bloom J. 2002. Early and widespread cholinergic losses differentiate dementia with Lewy bodies from Alzheimer disease. Arch Gen Psychiatry. 59:946–951.
Tomasi D, Wang RL, Telang F, Boronikolas V, Jayne MC, Wang GJ, Fowler JS, Volkow ND. 2009. Impairment of attentional networks after 1 night of sleep deprivation. Cereb Cortex. 19:233–240.
Valenzuela MJ, Sachdev P. 2001. Magnetic resonance spectroscopy in AD. Neurology. 56:592–598.
Van Der Werf YD, Weerts JG, Jolles J, Witter MP, Lindeboom J, Scheltens P. 1999. Neuropsychological correlates of a right unilateral lacunar thalamic infarction. J Neurol Neurosurg Psychiatry. 66:36–42.
Volkow N, Wang G, Hitzemann R, Fowler J, Pappas N, Lowrimore P, Burr G, Pascani K, Overall J, Wolf A. 1995. Depression of thalamic metabolism by lorazepam is associated with sleepiness. Neuropsychopharmacology. 12:123–132.
Walker MP, Ayre GA, Cummings JL, Wesnes K, McKeith IG, O'Brien JT, Ballard CG. 2000. The clinician assessment of fluctuation and the one day fluctuation assessment scale. Two methods to assess fluctuating confusion in dementia. Br J Psychiatry. 177:252–256.
Ward LM. 2011. The thalamic dynamic core theory of conscious experience. Conscious Cogn. 20:464–486.
Watson R, Blamire AM, Colloby SJ, Wood JS, Barber R, He J, O'Brien JT. 2012. Characterizing dementia with Lewy bodies by means of diffusion tensor imaging. Neurology. 79:906–914.
Wesnes KA, McKeith I, Edgar C, Emre M, Lane R. 2005. Benefits of rivastigmine on attention in dementia associated with Parkinson disease. Neurology. 65:1654–1656.
World Health Organization. 1992. The ICD-10 Classification of Mental and Behavioural Disorders. Geneva: World Health Organization.
Wurtman RJ, Blusztajn JK, Marie JC. 1985. Autocannibalism of choline-containing membrane phospholipids in the pathogenesis of Alzheimer's disease. Neurochem Int. 7:369–372.
Zarei M, Patenaude B, Damoiseaux J, Morgese C, Smith S, Matthews PM, Barkhof F, Rombouts SA, Sanz-Arigita E, Jenkinson M. 2010. Combining shape and connectivity analysis: an MRI study of thalamic degeneration in Alzheimer's disease. Neuroimage. 49:1–8.